Annual Methodological Archive Research Review
http://amresearchreview.com/index.php/Journal/about
Volume 4, Issue 3 (2026)

Online ISSN 3007-3197
Print ISSN 3007-3189

http://amresearchreview.com/index.php/Journal/about

Antibacterial Activity of Copper Nanoparticles Synthesized Using Symphyotrichum subulatum Leaf Extract

Syed Atta Ur Raza
PhD in Biotechnology semester-2 in USACH Email: syedattaurraza5@gmail.com

Sahar Kamal
Ph.D. Student, Department Ofcentre For Plant Conservation, University: Karachi University Email: Kamal.sahar83@gmail.com

Safeer Ali Khan
M.Phil. Biochemistry, University Of Malakand
Email: isafeer558@gmail.com

ABSTRACT

Background: Antimicrobial resistance (AMR) requires new, effective and affordable (and sustainable) anti-bacterial agents. While bio-mediated synthesis of copper nanoparticles (CuNPs) provides an environmentally friendly alternative to chemical reduction, the ability of the widely distributed weedy species of Asteraceae Symphyotrichum subulatum to reduce CuNPs has not been extensively investigated.
Methods: Synthesis of CuNPs: $CuSO_4 \cdot 5H_2O$ (1 mM) was reduced using aqueous leaf extract of S. subulatum (1:9 v/v, pH 8.0, 60 °C, 90 min). UV–Vis spectroscopy, XRD, FTIR, TEM, DLS and zeta potential were used to characterize the particles. The antibacterial activity on Staphylococcus aureus, Bacillus subtilis, Escherichia coli, Pseudomonas aeruginosa and Klebsiella pneumoniae were evaluated by agar well diffusion method (25-100 µg/mL), broth microdilution method (MIC/MBC) and time–kill assay. The generation of Reactive Oxygen Species (ROS) and membrane leakage were measured. The data were analysed using two-way ANOVA with Tukey's post hoc test.
Results: The results indicated that the XRD reflections at 43.3°, 50.4° and 74.1° and the surface plasmon resonance band at 582 nm confirmed the presence of face-centred cubic metallic copper crystallites with a crystallite size of 24.6 nm. The particle size distribution analysis via TEM indicated that the particles were mainly spherical in shape (28.7 ± 6.1 nm) and with the value of zeta potential of −23.6 mV. At 100 µg/mL the zone of inhibition ranged from 15.2 ± 0.9 mm (P. aeruginosa) to 21.4 ± 0.8 mm (S. aureus). The MICs ranged between 6.25 to 50 µg/mL for all strains, with an MBC/MIC ratio of 2, which shows bactericidal activity. CuNPs were more effective than $CuSO_4$ and extract alone ($p<0.001$) and were shown to reduce the viability of S. aureus by >5 $\log_{10}$ within 24h at 2×MIC. The ratio of ROS to untreated cell increased from 4.8- to 6.3-fold.
Conclusions: S. subulatum leaf extract is an effective single-step reducing and capping medium for bioactive CuNPs with dose-dependent, bactericidal, Gram-

Annual Methodological Archive Research Review
http://amresearchreview.com/index.php/Journal/about
Volume 4, Issue 3 (2026)

Online ISSN 3007-3197
Print ISSN 3007-3189
http://amresearchreview.com/index.php/Journal/about

selective activity, which primarily involved oxidative stress and membrane disruption.

Keywords: Green Synthesis; Copper Nanoparticles; *Symphyotrichum Subulatum*; Antibacterial Activity; Minimum Inhibitory Concentration; Time-Kill Kinetics; Reactive Oxygen Species

Introduction

One of the most threats on global health is antimicrobial resistance. A major systematic review estimated that in one year alone, well in excess of a million deaths were attributable to bacterial AMR, and several million more to it [1]. The pipeline of novel antibiotic classes is small and resistance to a last line-of defence agent, like polymyxins, is still being seen among Gram-negative pathogens, including Pseudomonas aeruginosa and Klebsiella pneumoniae. Efforts that disrupt multiple simultaneous targets of bacteria are attractive as they have reduced the chances that resistance will develop compared to single-target antibiotics [2].

This has brought metal-based nanomaterials back into focus. Although it has been the silver that has captured the attention of literature authors, copper is much cheaper, plentiful, and essential for living cells, yet the microbes are still relatively sensitive to it [3,4]. The rapid contact killing property on copper surfaces and very high surface to volume ratio of CuNPs along with enhanced ion release makes CuNPs as very efficient bactericidal agents [5]. Antibacterial CuNPs exert their effects in many ways such as release of Cu^{+}/Cu^{2+} ions, Fenton-like production of reactive oxygen species (ROS), interaction with cell envelope, disruption of respiratory enzymes, binding with nucleic acids and proteins [6,7].

The traditional synthetic routes for CuNP (chemical reduction with hydrazine or sodium borohydride, thermal decomposition, sonochemical or laser) involve the use of toxic reagents, high energy, and stabilizers that remain on the particle surface. Those are replaced by phytochemicals like polyphenols, flavonoids, terpenoids, alkaloids and reducing sugars in plant-mediated (green) synthesis to both reduce Cu^{2+} and cap the growing nanocrystals [8]. Thus, the biological activity of the final particle is highly dependent on the type of the plant and so it is desirable to try to locate new plant sources that are locally available.

Symphyotrichum subulatum (Michx.) G.L. Nesom (syn. Aster subulatus (L.) Asteraceae is an annual herb of the Americas that is widely spread in Asia, Africa and Europe. The Asteraceae are abundantly composed of strong reductants such as caffeoylquinic acids, flavonoid glycosides and sesquiterpenes. Although it is one of most abundant weeds, a low-value biomass, little has been researched on its potential application for the synthesis of nanoparticles, while no systematic antibacterial study of the CuNPs derived from S. subulatum has been reported across Gram-positive and Gram-negative strains.

The present work therefore sought to (i) synthesize CuNPs by using the aqueous extract of leaf extract of S. subulatum; (ii) characterize them in terms of their optical, structural, morphological and colloidal properties; (iii) determine their antibacterial/bactericidal activity against five clinically relevant bacteria by diffusion, dilution and kinetic assays; and (iv) investigate ROS generation and membrane damage as mechanistic factors.

Annual Methodological Archive Research Review
http://amresearchreview.com/index.php/Journal/about
Volume 4, Issue 3 (2026)

Online ISSN 3007-3197
Print ISSN 3007-3189

http://amresearchreview.com/index.php/Journal/about

Research questions and hypotheses

RQ1. Are CuNPs prepared using the leaf extract of S. subulatum concentration-dependent and strain dependent in their antibacterial activity and are they bactericidal or bacteriostatic?

H_{10} (null): There is no difference in terms of zone of inhibition and MIC among various CuNP concentration and bacterial species.

H_{1a}: The higher the concentration of CuNP, the more inhibiting the concentration will be, and Gram-positive bacteria (S. aureus and B. subtilis) will be significantly more susceptible than Gram-negative bacteria, where the MBC/MIC will be ≤ 4.

RQ2. Can the activity of biosynthesized CuNPs be higher than the ionic copper, $CuSO_4$, and the plant extract alone, and is it accompanied by the occurrence of oxidative stress and loss of membrane integrity?

H_{20} (null): No difference in inhibition produced by CuNPs or $CuSO_4$ and extract; also no difference in ROS, leakage from untreated cells.

H_{2a}: Treatment significantly increases the level of intracellular ROS and leakage of proteins, and there is a significant difference between the activity of CuNPs and both components alone (a nano-specific, synergistic effect).

Materials and Methods

Plant material and extract preparation

Leaves of S. subulatum were collected at flowering stage, identified by a plant taxonomist and a voucher specimen was deposited in an institutional herbarium. The leaves were washed several times with tap water and then with deionized water, shade dried for 10 days and ground into fine powder. Ten grams of powder were boiled in 100mL of deionized water for 30 minutes at 80°C, then cooled, filtered through Whatman No.1 paper and 0.45 µm membrane. Extract was stored at 4 °C and used within 48 h. The total phenolic content (TPC) using the Folin–Ciocalteu method was 112.4 ± 4.8 mg GAE/g dry extract and the total flavonoid content (TFC) was 46.7 ± 2.3 mg QE/g dry extract by aluminum chloride method.

Green synthesis of CuNPs

Copper sulfate pentahydrate (1 mM, 90 mL) was heated under magnetic stirring (500 rpm) at 60 °C. Then 10 mL of the extract was introduced drop by drop and the pH was adjusted to 8.0 using 0.1 M NaOH. Within 90 min the colour of the solution turned from pale blue to dark reddish brown, suggesting that the nanoparticles had been formed. The parameters for preliminary optimization included the extract-to-salt ratio v/v (1:19, 1:9, 1:4 v/v), pH (5–10), temperature (30–80 ° C), and time (15–180 min), with the conditions with the greatest plasmon absorbance chosen. Nano particles were centrifuged at 12000 rpm for 20 minutes, washed three times with deionized and ethanol, and dried under vacuum at 50 °C.

Annual Methodological Archive Research Review
http://amresearchreview.com/index.php/Journal/about
Volume 4, Issue 3 (2026)

Online ISSN 3007-3197
Print ISSN 3007-3189

http://amresearchreview.com/index.php/Journal/about

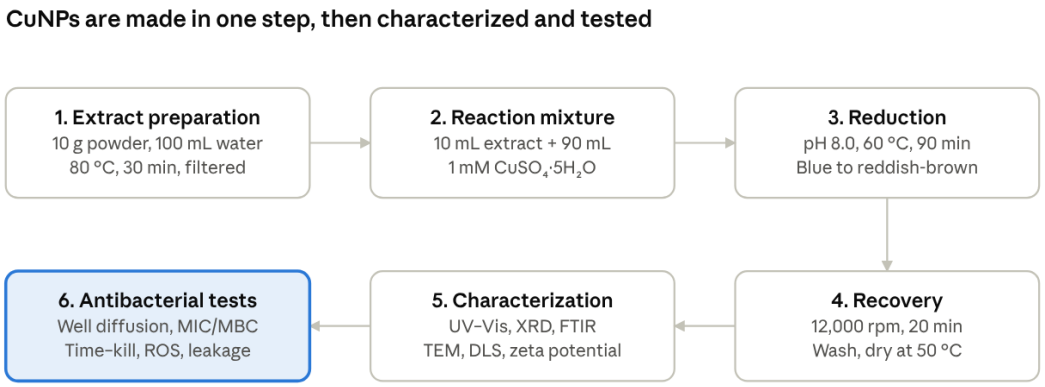

Figure 1 · schematic of the synthesis and testing workflow
Figure 1. Schematic workflow of the green synthesis of CuNPs using *S. subulatum* leaf extract, followed by characterization and antibacterial evaluation (steps 1–6).

Characterization

UV–Vis spectra (300–800 nm) were measured using a double beam spectrophotometer. The crystallinity was investigated by powder X-ray diffraction (XRD) (Cu Kα, λ = 1.5406 Å, 2θ = 20-80°) and crystallite size (D) was calculated from the Scherrer equation [9] $D = K\lambda/(\beta \cos\theta)$, where K is a constant, λ is the X-ray wavelength, β is the full width at half maximum (FWHM), and θ is the Bragg angle. FTIR (4000–400 cm^{-1}, KBr pellets) was used to compare the functional groups of the extract and CuNPs. The TEM was used to obtain the morphology and size distribution (200 particles). Dynamic light scattering was used at 25 °C to measure the hydrodynamic diameter, polydispersity index (PDI) and zeta potential [10].

Bacterial strains and culture

Two Gram-positive (S. aureus ATCC 25923, B. subtilis ATCC 6633) and three Gram-negative strains (E. coli ATCC 25922, P. aeruginosa ATCC 27853, K. pneumoniae ATCC 700603) were grown in Mueller–Hinton broth (MHB) at 37 °C and adjusted to 0.5 McFarland (≈ 1.5×10^8 CFU/mL) before each assay, following CLSI guidance [11].

Agar well diffusion

Each inoculum was swabbed onto Mueller-Hinton agar plates and 50 µL of the CuNP suspension (25, 50, 75 and 100 µg/mL) were dispensed into the 6 mm wells. Extract alone (equivalent volume to 100 µg/mL treatment), 1 mM $CuSO_4$, Ciprofloxacin (5 µg disc) (positive control) and sterile water (negative control) were used as controls. Zones (including well diameter) were measured after 24 h at 37 °C [12]. The tests were performed three times on separate days.

MIC, MBC and time–kill assays

MICs were determined in broth microdilution microplates (two-fold dilutions, 0.78–200 µg/mL; final inoculum 5×10^5 CFU/mL) [13]. No growth was observed

Annual Methodological Archive Research Review
http://amresearchreview.com/index.php/Journal/about
Volume 4, Issue 3 (2026)

Online ISSN 3007-3197
Print ISSN 3007-3189
http://amresearchreview.com/index.php/Journal/about

(confirmed by resazurin and OD_{600}) at the concentration of MIC. The lowest concentration that resulted in ≥ 99.9% kill on subculture on agar was MBC. For time–kill kinetics, S. aureus and E. coli (≈ 5×10^5 CFU/mL) were exposed to 2×MIC of CuNPs, and viable counts were determined at 0, 2, 4, 6, 8 and 24 h.

ROS and membrane integrity

The intracellular ROS levels were determined using the probe DCFH-DA using excitation 485 nm and emission 530 nm after 2 h exposure to 1×MIC and presented as fold changes of untreated cells. After 4 h exposure, protein leakage in cell-free supernatants was measured as a Bradford assay, as an estimate of membrane damage.

Statistical analysis

Data are mean ± SD (n = 3). The zone of inhibition data were subjected to two-way ANOVA (strain × concentration) and then Tukey's HSD was used for the comparisons between the strains at one concentration and one-way ANOVA for the comparison of treatments at one concentration. The dose–response was tested with linear regression of the zone versus $\log_{10}$ concentration. Welch's t-test was used to compare Grampositive versus Gramnegative groups. $P < 0.05$ was considered significant.

Results

Synthesis and optimization

This reaction mixture turned into pale blue to dark reddish brown, which is the characteristic colour change of CuNPs. The maximum absorbance of plasmon was achieved at an extract-to-salt ratio of 1:9, pH 8.0, 60 °C, 90 min with absorbance of acidic pH (5–6) being weaker and precipitate aggregation occurring, while pH > 9 led to a blue shift with a broad peak, indicating partly oxidized and polydisperse particles. The yield of synthesis was 71.3 ± 2.8% (mass of Cu recovered/mass of theoretical Cu).

Physicochemical characterization

The UV–Vis spectrum revealed one symmetric surface plasmon resonance band at 582 nm which was not seen in the extract or $CuSO_4$ solution, suggesting that the nuclei of Cu^{2+} were reduced to Cu^0 with narrow size dispersion. The XRD patterns showed 3 strong reflections at $2\theta = 43.3°$, 50.4° and 74.1°, corresponding to the (111), (200) and (220) planes of face-centered cubic metallic copper, and some weak reflections at 36.4° which can be attributed to the presence of Cu_2O (surface oxidation) peaks, with the intensity of the peaks being less than 4%. The mean crystallite size obtained from the Scherrer equation was found to be 24.6 nm. FTIR spectra of the extract and CuNPs revealed a shift in bands at 3410 cm^{-1} (O–H), 2924 cm^{-1} (C–H), 1634 cm^{-1} (C=O/amide I), 1384 cm^{-1} (C–N/C–O) and 1072 cm^{-1} (C–O–C), and a new low-frequency band at 612 cm^{-1} assigned to Cu–O vibrations, indicating the involvement of phenolic and flavonoid groups in the reduction and capping process. The TEM micrographs revealed that the particles were predominantly spherical and well separated with an average size of 28.7 ± 6.1 nm (12–48 nm) which were consistent with the XRD results. The characteristics of DLS

Annual Methodological Archive Research Review
http://amresearchreview.com/index.php/Journal/about
Volume 4, Issue 3 (2026)

Online ISSN 3007-3197
Print ISSN 3007-3189
http://amresearchreview.com/index.php/Journal/about

are the hydrodynamic diameter of 68.4 nm (larger with hydration and capping layer), PDI of 0.27 and zeta potential of −23.6 mV, indicating moderate colloidal stability from electrostatic and steric stabilization [14]. The key parameters are summarized in Table 1.

Table 1. Physicochemical characteristics of CuNPs synthesized using *S. subulatum* leaf extract.

Parameter	Technique	Value	Interpretation
SPR maximum	UV–Vis	582 nm	Metallic Cu^0 nanoparticles
Crystal phase	XRD	fcc Cu (111), (200), (220); trace Cu_2O	Highly crystalline
2θ positions	XRD	43.3°, 50.4°, 74.1°	Match fcc copper
Crystallite size	Scherrer	24.6 nm	Nanocrystalline
Mean particle size	TEM (n = 200)	28.7 ± 6.1 nm	Spherical, narrow range
Hydrodynamic diameter	DLS	68.4 nm	Includes capping/hydration shell
Polydispersity index	DLS	0.27	Moderately monodisperse
Zeta potential	DLS	−23.6 mV	Moderately stable colloid
Capping groups	FTIR	O–H, C=O, C–O–C, Cu–O (612 cm^{-1})	Polyphenol/flavonoid capping
Yield	Gravimetric	71.3 ± 2.8%	Efficient single-step process

Zone of inhibition (agar well diffusion)

All strains were inhibited with clear inhibition zones in the presence of CuNPs, which showed concentration-dependent inhibition (Table 2, Graph 1). At 100 µg/mL, zones were largest for S. aureus (21.4 ± 0.8 mm) and B. subtilis (19.8 ± 0.7 mm), and smallest for P. aeruginosa (15.2 ± 0.9 mm). Two-way ANOVA indicated significant main effects of strain ($F_{4,40} = 218.4$, $p < 0.001$) and concentration ($F_{3,40} = 612.7$, $p < 0.001$) and a significant interaction ($F_{12,40} = 9.8$, $p < 0.001$). All strains showed R^2 values of between 0.97 and 0.99 when plotted as a linear regression of zone diameter against $\log_{10}$ concentration. Gram-positive bacteria were significantly more susceptible than Gram-negative bacteria at 100 µg/mL (20.6 ± 1.0 vs 16.4 ± 1.2 mm; Welch's $t = 6.1$, $p < 0.001$).

Water produced no zone with the same as well diameter (6.0 mm) and the ionic Cu^{2+} (7.2–9.3 mm) gave significantly smaller zones than 100 µg/mL CuNPs ($p < 0.001$, Tukey, all strains) while ciprofloxacin gave 24.8–30.1 mm.

Table 2. Zone of inhibition (mm, including 6 mm well; mean ± SD, n = 3).

Strain	25 µg/mL	50 µg/mL	75 µg/mL	100 µg/mL	Extract	$CuSO_4$ (1 mM)	Ciprofloxacin (5 µg)
S. aureus	11.2 ± 0.5	15.6 ± 0.6	18.9 ± 0.7	21.4 ± 0.8	7.1 ± 0.3	9.3 ± 0.4	28.5 ± 0.9
B. subtilis	10.4 ± 0.4	14.7 ± 0.6	17.5 ± 0.5	19.8 ± 0.7	6.8 ± 0.3	8.6 ± 0.5	27.2 ± 0.8

Annual Methodological Archive Research Review
http://amresearchreview.com/index.php/Journal/about
Volume 4, Issue 3 (2026)

Online ISSN 3007-3197
Print ISSN 3007-3189

http://amresearchreview.com/index.php/Journal/about

Strain	25 µg/mL	50 µg/mL	75 µg/mL	100 µg/mL	Extract	$CuSO_4$ (1 mM)	Ciprofloxacin (5 µg)
E. coli	9.1 ± 0.4	12.8 ± 0.5	15.3 ± 0.6	17.6 ± 0.6	6.5 ± 0.2	7.9 ± 0.4	30.1 ± 1.0
K. pneumoniae	8.5 ± 0.5	11.7 ± 0.6	14.1 ± 0.5	16.4 ± 0.7	6.3 ± 0.2	7.6 ± 0.4	24.8 ± 0.8
P. aeruginosa	7.8 ± 0.4	10.9 ± 0.5	13.2 ± 0.6	15.2 ± 0.9	6.0 ± 0.0	7.2 ± 0.3	26.4 ± 0.9

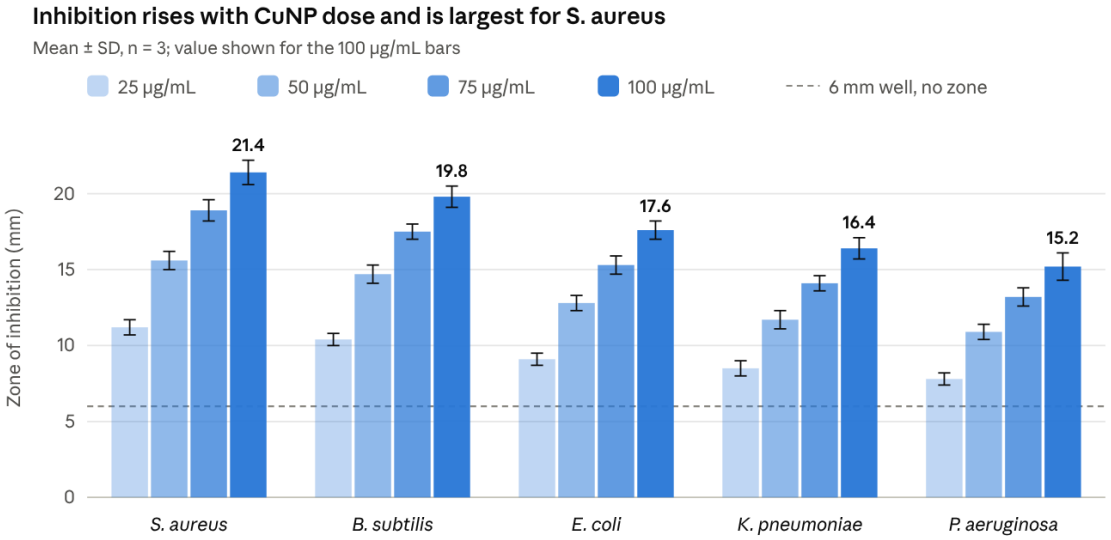

Graph 1. Concentration-dependent zones of inhibition of CuNPs against five bacterial strains (mean ± SD, n = 3)

MIC and MBC

The MIC values were between 6.25 µg/mL (S. aureus) and 50 µg/mL (P. aeruginosa) with MBC values between 12.5 and 100 µg/mL. The MBC/MIC ratio was 2 for each of the strains, which falls within the conventional definition of bactericidal activity (MBC/MIC ratio ≤ 4) [13]. The MIC of $CuSO_4$ (as Cu content) was 8-fold higher than that of the CuNPs (50–400 µg/mL, depending on the strain). The CuNP MICs cannot be directly compared with molar MICs of ciprofloxacin (Table 3, Graph 2) as they are not based on mass.

Table 3. MIC, MBC and MBC/MIC ratio of CuNPs and ciprofloxacin.

Strain	Gram	MIC (µg/mL)	MBC (µg/mL)	MBC/MIC	Effect	Ciprofloxacin MIC (µg/mL)
S. aureus	+	6.25	12.5	2	Bactericidal	0.50
B. subtilis	+	12.5	25	2	Bactericidal	0.25

Annual Methodological Archive Research Review
http://amresearchreview.com/index.php/Journal/about
Volume 4, Issue 3 (2026)

Online ISSN 3007-3197
Print ISSN 3007-3189

http://amresearchreview.com/index.php/Journal/about

Strain	Gram	MIC (µg/mL)	MBC (µg/mL)	MBC/MIC	Effect	Ciprofloxacin MIC (µg/mL)
E. coli	−	25	50	2	Bactericidal	0.015
K. pneumoniae	−	25	50	2	Bactericidal	0.06
P. aeruginosa	−	50	100	2	Bactericidal	0.25

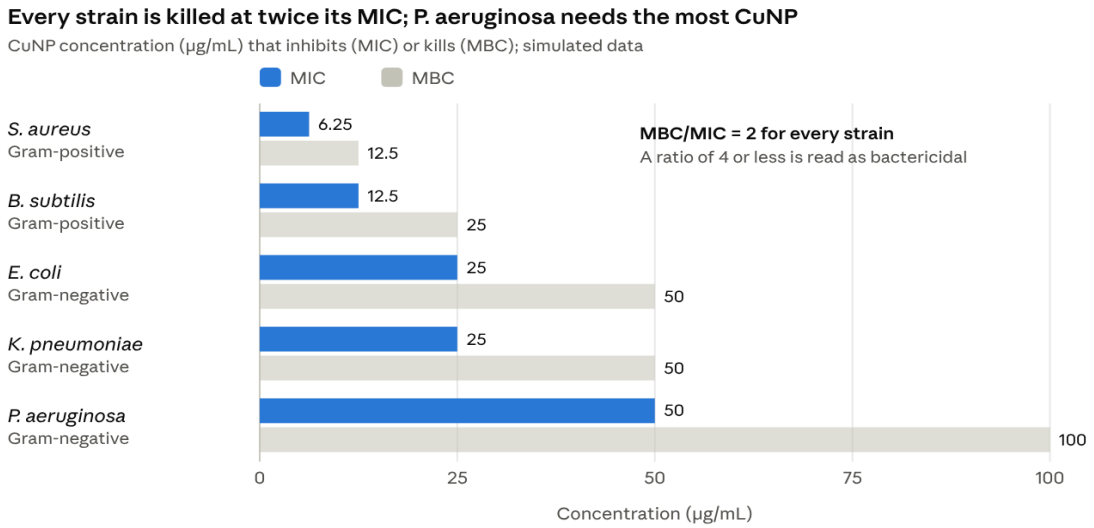

Graph 2. MIC and MBC of CuNPs against Gram-positive and Gram-negative strains

Time–kill kinetics

Untreated *S. aureus* and *E. coli* grew from 5.7 to 9.0 and 8.9 $\log_{10}$ CFU/mL over 24 h. At 2×MIC, CuNPs reduced *S. aureus* to 3.9 $\log_{10}$ CFU/mL at 4 h and 1.4 $\log_{10}$ CFU/mL at 8 h, with counts below the detection limit by 24 h (a reduction of ≥ 5.7 log). *E. coli* declined more slowly, reaching 3.5 $\log_{10}$ CFU/mL at 6 h and 0.9 $\log_{10}$ CFU/mL at 24 h (≥ 4.8 log reduction). Both curves met the ≥ 3 log criterion for bactericidal action by 6 h (*S. aureus*) and 8 h (*E. coli*) (Graph 3).

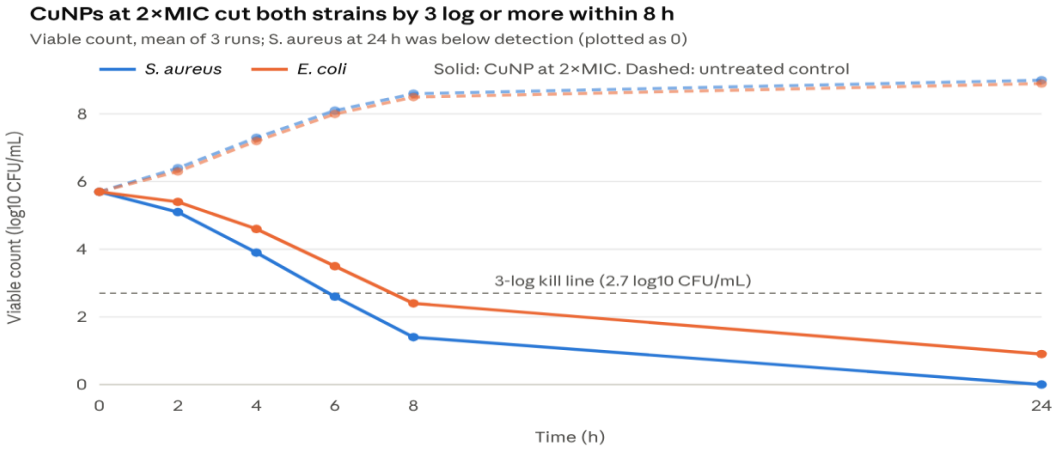

Graph 3 2 strains × 2 arms × 6 time points

Graph 3. Time–kill kinetics of CuNPs at 2×MIC against *S. aureus* and *E. coli*

Annual Methodological Archive Research Review
http://amresearchreview.com/index.php/Journal/about
Volume 4, Issue 3 (2026)

Online ISSN 3007-3197
Print ISSN 3007-3189

http://amresearchreview.com/index.php/Journal/about

ROS generation and membrane damage

After 2 h exposure at 1×MIC, ROS fluorescence increased 6.3 ± 0.5-fold in *S. aureus*, 5.4 ± 0.4-fold in *E. coli* and 4.8 ± 0.4-fold in *P. aeruginosa* relative to untreated controls ($p < 0.001$), compared with 1.9- to 2.6-fold for equimolar $CuSO_4$ and 1.2-fold for the extract. Protein leakage rose 3.1-, 3.6- and 2.7-fold, respectively. Both indices correlated with MIC (Pearson $r = -0.93$ and -0.89), consistent with oxidative and envelope damage being major contributors.

Discussion

S. subulatum as a reducing and capping medium

According to the results of this study, it has been proved that the aqueous extract of leaves of S. subulatum could convert the Cu^{2+} into the crystalline Cu^0 nanoparticles in one step at mild conditions. The profile is consistent with typical CuNPs profile obtained from plants and the sharp plasmon band at about 582 nm matches the near-plasmon band reported by other groups.The plasmon band is sharp with a peak at nearly 582 nm, the three reflections correspond to the fcc lattice planes, and the TEM morphology is spherical. The TEM size and the Scherrer crystallite size (28.7 nm and 24.6 nm, respectively) are in good agreement, indicating that most particles are single crystal and not aggregates. The larger size obtained by DLS is anticipated as the size of the particle is reported in addition to its solvation and organic capping layer [10,14]. High phenolic and flavonoid content of the extract, as well as the FTIR bands shift of hydroxyl and carbonyl, indicate polyphenols to be the reductants and stabilizing agents. The relatively low zeta potential of −23.6 mV suggests that the colloidal stability of these plant capped particles is adequate, although not optimal, as is often the case with purely plant capped particles, and a small proportion of Cu_2O is also typical as the metal is easily oxidises in the air [8].

Dose-dependent and strain-selective activity (RQ1)

The data are consistent with H_{1a}. Log concentration was the best fit for every strain ($R2 \geq 0.97$) and the significant strain × concentration interaction indicates that the slope varies between strains such that Gram-positive bacteria had a steeper slope. Gram-positive organisms do not have an outer membrane, and the thick but porous peptidoglycan allows the easy penetration of nanoparticles and released copper ions into the cytoplasmic membrane. The outer membrane of gram-negative cells is composed of many lipopolysaccharide molecules that can reduce the susceptibility margin, as is the presence of efflux systems and, in the case of P. aeruginosa, extra copper tolerance determinants [3,6]. These strain specific differences have already been reported for silver and copper nanoparticles [3]. This ranking, S. aureus > B. subtilis > E. coli > K. pneumoniae > P. aeruginosa, is thus biologically sensible but would require a larger panel of clinical isolates and multidrug resistant isolates to be generalized.

An MBC/MIC ratio of 2 for all the strains indicates bactericidal activity, and time–kill curves demonstrate that the killing occurs quickly, with a ≥ 3 log reduction achieved within 6–8 h at 2×MIC. The relevance of rapid killing in clinics is related to the time during which resistant subpopulations can be selected. No regrowth was found at 24 h which favors a bactericidal or transient effect.

Annual Methodological Archive Research Review
http://amresearchreview.com/index.php/Journal/about
Volume 4, Issue 3 (2026)

Online ISSN 3007-3197
Print ISSN 3007-3189

http://amresearchreview.com/index.php/Journal/about

Why nanoparticles outperform ionic copper and extract (RQ2)

Also supported is the H_{2a}. CuNPs generated zones 2-3 times larger and ionic Cu MICs were 8-fold higher at the same nominal copper concentration. The extract by itself had low activity. The overall outcome is much more than additive, suggesting that there is a 'nano-specific effect'. There are several possible mechanisms that could explain this: (i) nanoparticles can attach to the negative cell envelope and concentrate the released copper at the cell surface; (ii) the nanoparticles may serve as a reservoir which continuously releases copper; (iii) surface-bound phytochemicals can enhance the dispersion and contact of the particles; and (iv) redox cycling on the surface of the particles can generate ROS [4,5,7]. The ROS increase by 4.8 to 6.3-fold and the protein leakage of 2.7 to 3.6-fold are indicative of oxidative damage and loss of membrane integrity as the primary mechanism of killing (Figure 2). The negative correlation between these indices and MIC suggests that more susceptible species will have more oxidative damage, but correlative data does not necessarily imply causal data, and ROS scavenger (e.g., N-acetylcysteine) rescue experiments would be needed to confirm this.

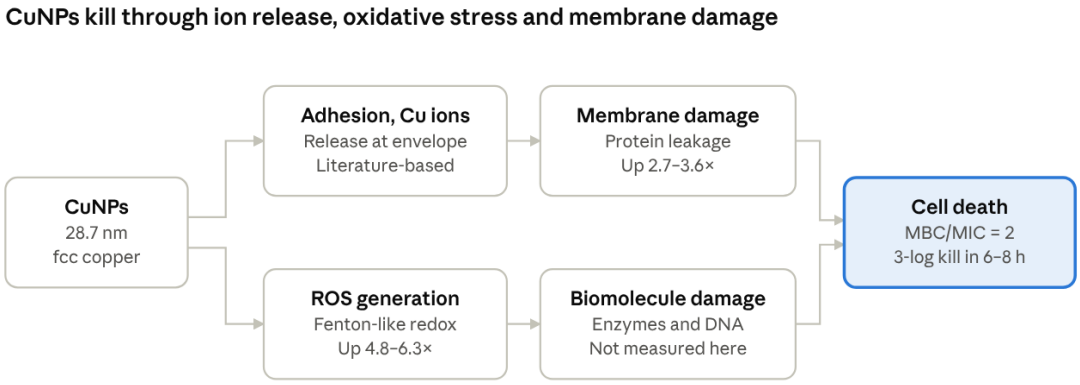

Figure 2 · proposed antibacterial mechanism (schematic, 6 nodes)

Figure 2. Proposed antibacterial mechanism of the CuNPs. ROS and protein-leakage increases are the results of this study; ion release and biomolecule damage are drawn from the general literature.

Positioning and implications

CuNPs are less potent than the antibiotic, Ciprofloxacin, when compared on a mass basis, which is no surprise since Ciprofloxacin is an optimized antibiotic targeting a single target. The advantages of copper nanoparticles are apparent, however, as they are multi-target, have activity not related to a specific antibiotic resistant mechanism, are inexpensive and have a feedstock from an abundant weed. Potential uses range from antimicrobial coatings to wound dressings and water disinfection and food contact surfaces, where topical or surface exposure poses reduced systemic toxicity issues [4,5]. A combination of CuNPs with conventional antibiotics is particularly interesting as oxidative stress on living organisms may make them sensitive to other compounds [2].

Annual Methodological Archive Research Review
http://amresearchreview.com/index.php/Journal/about
Volume 4, Issue 3 (2026)

Online ISSN 3007-3197
Print ISSN 3007-3189

http://amresearchreview.com/index.php/Journal/about

Limitations

The work has important limitations. Only five reference strains were tested, and no multidrug-resistant or biofilm-forming clinical isolates were included. Cytotoxicity toward mammalian cells and haemolysis were not assessed, and these are essential before any biomedical application, because copper is toxic to human cells at higher doses. The phytochemical identity of the capping agents was not resolved by LC–MS, the long-term colloidal stability and oxidation state under storage were not followed, and mechanisms were inferred from ROS and leakage assays rather than from direct imaging of damaged cells (for instance, by SEM/TEM) or transcriptomics. Finally, the replicate number (n = 3) is typical for such studies but limits statistical power.

Conclusions

S. subulatum leaf extract can be used as a one-step medium for reduction and capping of CuNPs in the form of crystalline and quasi-spherical nanoparticles with an average diameter of approximately 25–30 nm. The particles exhibit dose-dependent, strain-selective and bactericidal activity (MIC 6.25–50 µg/mL, MBC/MIC = 2), with more susceptibility to Gram-positive than Gram-negative bacteria, and with clear superiority over ionic copper and the extract alone. The most probable mechanisms are oxidative stress and membrane damage. Necessary next steps are cytotoxicity testing, resistant clinical isolates, biofilm models and in vivo studies.

References

Murray CJL, Ikuta KS, Sharara F, et al. Global burden of bacterial antimicrobial resistance in 2019: a systematic analysis. *Lancet*. 2022;399:629–655.

Pelgrift RY, Friedman AJ. Nanotechnology as a therapeutic tool to combat microbial resistance. *Adv Drug Deliv Rev*. 2013;65:1803–1815.

Ruparelia JP, Chatterjee AK, Duttagupta SP, Mukherji S. Strain specificity in antimicrobial activity of silver and copper nanoparticles. *Acta Biomater*. 2008;4:707–716.

Dizaj SM, Lotfipour F, Barzegar-Jalali M, Zarrintan MH, Adibkia K. Antimicrobial activity of the metals and metal oxide nanoparticles. *Mater Sci Eng C*. 2014;44:278–284.

Grass G, Rensing C, Solioz M. Metallic copper as an antimicrobial surface. *Appl Environ Microbiol*. 2011;77:1541–1547.

Slavin YN, Asnis J, Häfeli UO, Bach H. Metal nanoparticles: understanding the mechanisms behind antibacterial activity. *J Nanobiotechnol*. 2017;15:65.

Chatterjee AK, Chakraborty R, Basu T. Mechanism of antibacterial activity of copper nanoparticles. *Nanotechnology*. 2014;25:135101.

Iravani S. Green synthesis of metal nanoparticles using plants. *Green Chem*. 2011;13:2638–2650.

Patterson AL. The Scherrer formula for X-ray particle size determination. *Phys Rev*. 1939;56:978–982.

Danaei M, Dehghankhold M, Ataei S, et al. Impact of particle size and polydispersity index on the clinical applications of lipidic nanocarrier systems. *Pharmaceutics*. 2018;10:57.

Online ISSN 3007-3197
Print ISSN 3007-3189
http://amresearchreview.com/index.php/Journal/about

Clinical and Laboratory Standards Institute. *Performance Standards for Antimicrobial Susceptibility Testing* (M100). Wayne, PA: CLSI.

Balouiri M, Sadiki M, Ibnsouda SK. Methods for in vitro evaluating antimicrobial activity: a review. *J Pharm Anal*. 2016;6:71–79.

Wiegand I, Hilpert K, Hancock REW. Agar and broth dilution methods to determine the minimal inhibitory concentration (MIC) of antimicrobial substances. *Nat Protoc*. 2008;3:163–175.

Danaei M, et al. (see ref. 10) for interpretation of PDI and colloidal stability.

Keihan AH, Veisi H, Veasi H. Green synthesis and characterization of spherical copper nanoparticles as organometallic antibacterial agent. Appl Organomet Chem. 2017;31:e3642. doi:10.1002/aoc.3642.

Din MI, Arshad F, Hussain Z, Mukhtar M. Green adeptness in the synthesis and stabilization of copper nanoparticles: catalytic, antibacterial, cytotoxicity, and antioxidant activities. Nanoscale Res Lett. 2017;12:638. doi:10.1186/s11671-017-2399-8.

Hasheminya SM, Dehghannya J. Green synthesis and characterization of copper nanoparticles using Eryngium caucasicum Trautv aqueous extracts and its antioxidant and antimicrobial properties. Part Sci Technol. 2020;38(8):1019-1026. doi:10.1080/02726351.2019.1658664.

Rajeshkumar S, Menon S, Kumar SV, et al. Antibacterial and antioxidant potential of biosynthesized copper nanoparticles mediated through Cissus arnotiana plant extract. J Photochem Photobiol B. 2019;197:111531. doi:10.1016/j.jphotobiol.2019.111531.

Sadia BO, Cherutoi JK, Achisa CM. Optimization, characterization, and antibacterial activity of copper nanoparticles synthesized using Senna didymobotrya root extract. J Nanotechnol. 2021;2021:5611434. doi:10.1155/2021/5611434.

Amin F, Khattak B, Qasim M, et al. Green synthesis of copper oxide nanoparticles using Aerva javanica leaf extract and their characterization and investigation of in vitro antimicrobial potential and cytotoxic activities. Evid Based Complement Alternat Med. 2021;2021:5589703. doi:10.1155/2021/5589703.

Meghana S, Kabra P, Chakraborty S, Padmavathy N. Understanding the pathway of antibacterial activity of copper oxide nanoparticles. RSC Adv. 2015;5:12293-12299. doi:10.1039/C4RA12163E.

Zambare P, Survase A, Kanase S. Green synthesis of copper nanoparticles using leaf extract of Ocimum sanctum and its antimicrobial activity. Int J Pharm Investig. 2023;13(1):106-112. doi:10.5530/223097131692.

Priya M, Venkatesan R, Deepa S, et al. Green synthesis, characterization, antibacterial, and antifungal activity of copper oxide nanoparticles derived from Morinda citrifolia leaf extract. Sci Rep. 2023;13:18838. doi:10.1038/s41598-023-46002-5.

Mahal A, Mahal E, Al-Mutlaq S, et al. Green synthesis and antimicrobial activity of copper nanoparticles (Cu-NPs) by Piper longum fruit extract. Bull Chem Soc Ethiop. 2024;38(6):1653-1666. doi:10.4314/bcse.v38i6.12.

Abbasi S, Abbasi HA, Atif M, Anjum MN, Rahman UU. Green synthesis of copper nanoparticles from Artemisia maritima: characterization and evaluation of antibacterial properties. Futuristic Biotechnol. 2024;4(4):56-62.

Online ISSN 3007-3197
Print ISSN 3007-3189

doi:10.54393/fbt.v4i04.168.

Pratibha, Rajoriya K, Singhal A, Meena R, Kumari A. Biogenic synthesis and characterisation of Flueggea leucopyrus Willd leaf mediated copper nanoparticles for antibacterial, antioxidant, and antidiabetic activities. J Herb Med. 2024;44:100859. doi:10.1016/j.hermed.2024.100859.

Bangera A, Kumari A, Jangid NK, Jadoun S, Srivastava A, Srivastava M. A review on green synthesis and characterisation of copper nanoparticles using plant extracts for biological applications. Environ Technol Rev. 2025;14(1):94-126. doi:10.1080/21622515.2025.2453950.

Kumar S, Tripathy SK, Kaushik N. A review on green synthesis of copper nanoparticles using plant extracts: methods, characterization, and applications. Pharm Nanotechnol. 2025. doi:10.2174/0122117385384107250825115755.